

This article was downloaded by:

On: 30 January 2011

Access details: *Access Details: Free Access*

Publisher *Taylor & Francis*

Informa Ltd Registered in England and Wales Registered Number: 1072954 Registered office: Mortimer House, 37-41 Mortimer Street, London W1T 3JH, UK



Separation & Purification Reviews

Publication details, including instructions for authors and subscription information:

<http://www.informaworld.com/smpp/title~content=t713597294>

Modern Countercurrent Distribution

R. A. Barford^a

^a Eastern Regional Research Center Agricultural Research Service, USDA, Philadelphia, Pennsylvania

To cite this Article Barford, R. A.(1975) 'Modern Countercurrent Distribution', *Separation & Purification Reviews*, 4: 2, 351 — 397

To link to this Article: DOI: 10.1080/03602547508066044

URL: <http://dx.doi.org/10.1080/03602547508066044>

PLEASE SCROLL DOWN FOR ARTICLE

Full terms and conditions of use: <http://www.informaworld.com/terms-and-conditions-of-access.pdf>

This article may be used for research, teaching and private study purposes. Any substantial or systematic reproduction, re-distribution, re-selling, loan or sub-licensing, systematic supply or distribution in any form to anyone is expressly forbidden.

The publisher does not give any warranty express or implied or make any representation that the contents will be complete or accurate or up to date. The accuracy of any instructions, formulae and drug doses should be independently verified with primary sources. The publisher shall not be liable for any loss, actions, claims, proceedings, demand or costs or damages whatsoever or howsoever caused arising directly or indirectly in connection with or arising out of the use of this material.

MODERN COUNTERCURRENT DISTRIBUTION

R. A. Barford
Eastern Regional Research Center
Agricultural Research Service, USDA
Philadelphia, Pennsylvania 19118

Interest in liquid-liquid extraction continues to grow as evidenced by such divergent applications as industrial waste water treatment^{1,2} cleanup for pesticide residue analysis,³ and resolution of optical isomers.⁴ This activity results from increased understanding of the chemistry of solvent extraction which is leading to the design of specially selective systems^{4,5} as well as the development of improved extractors emanating from studies of mass transfer phenomena^{6,7} in continuously flowing systems.

Some interesting designs for laboratory preparative scale continuous extractors have been described. They include the "rocking" glass train of Hietala,⁸ the mixer-settler cells described by Anwar et al.,⁹ the rotating partitioned cylinder of Kovats,¹⁰ and the fibrous strand-two continuous phase system developed by Pan.¹¹ Countercurrent chromatography, a technique which combines the selectivity of liquid-liquid extraction with the efficiency and speed of column chromatography and which seems particularly suited for analysis of biological macromolecules has been reviewed recently in this journal by its developers.¹²

The effects of nonideal behavior in discontinuous automatic extractors such as those described by Craig,^{13,14} Alderweireldt,¹⁵ Wilhelm,¹⁶ Signer,¹⁷ and Albertsson¹⁸ has also been demonstrated. Recent applications of these devices include the isolation of biomedically important alkaloids,¹⁹ the fractionation of the five

component lactic acid dehydrogenase isozyme system,²⁰ and the preparation of molecularly homogeneous fractions of poly(ethoxy)-ethanols.²² The theory and practice of these discontinuous extractors will be discussed in this report.

Phase Equilibria and Solvent Selection

Separation depends on the differential partitioning of components in a mixture between two or more liquid phases. Many equilibrations and transfers through long trains of cells may be carried out conveniently with modern robot-controlled distributors which are capable, therefore, of resolving closely related components. In contrast to continuous extractors, equilibrium is usually reached and complete settling of phases obtained in each stage. At equilibrium in a two-phase system

$$(1) \quad \mu_{i,1} = \mu_{i,2} \text{ where } \mu_i = \left(\frac{\partial G_i}{\partial n_i} \right)_{T,P,n} \#$$

$$(2) \quad \Delta G^m = \sum_{i=1}^{\#} x_i (\mu_i - \mu_i^{\circ})$$

$$(3) \quad \mu_i - \mu_i^{\circ} = RT \ln a = RT (\ln x_i + \ln f_i)$$

$$(4) \quad \frac{\Delta G^m}{RT} = \sum_{i=1}^{\#} x_i \ln x_i + \sum_{i=1}^{\#} x_i \ln f_i$$

$$(5) \quad \sum_{i=1}^{\#} x_i d(\ln f_i) = 0 \quad (\text{Gibbs-Duhem relation})^{23,24}$$

The left summation in eq. (4) defines ideal behavior for all components and the right deviations from ideality. The latter is frequently called the excess free energy,²⁵ G^E . At least one of the component's (solvent's) activity coefficients (f) must be far from 1 ($a = 1$ for pure component) for phase separation to occur. In order for the other components (solute) to be distributed between the phases, their behavior cannot be ideal in each phase and their f 's may vary in a different manner in each phase.

This is shown diagrammatically in Figure 1 where the activity of solute in two solvents is sketched. Frequently the solute

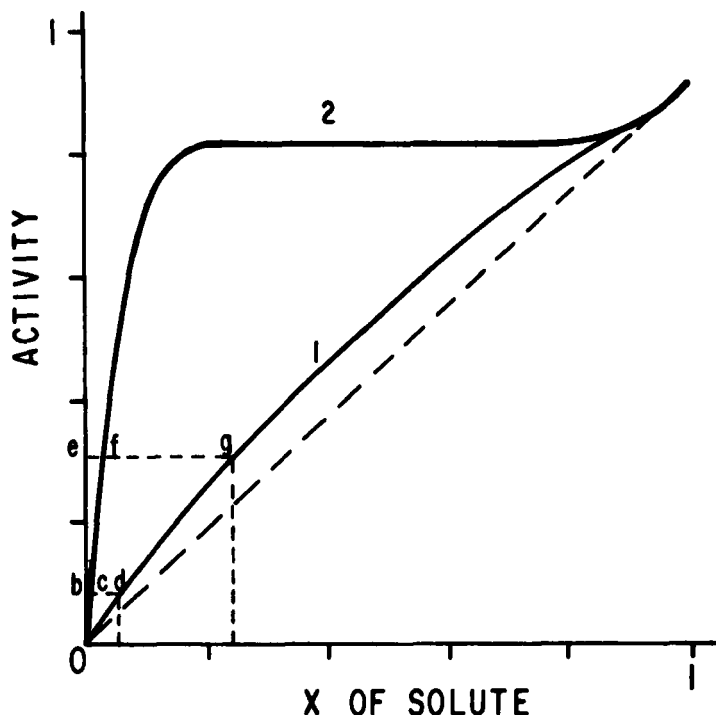


FIGURE 1

Hypothetical activity curves for a solute in two immiscible solvents. (1) better solvent (2) poorer solvent

itself is immiscible in one of the solvents. Curve (2) depicts such a condition (see also Figure 4-C). Since from eqs. (1) and (3), the activity of the solute is the same in both phases, the immiscible portion is seen as a horizontal line. Only the relative proportion of the phases varies in this region. The solute is completely soluble in solvent (1). From the curvature of (1) and (2), it is seen that the relationship:

$$(6) \quad \frac{x_{i,1}}{x_{i,2}} = \frac{\frac{a_{i,1}}{f_{i,1}}}{\frac{a_{i,2}}{f_{i,2}}} = \frac{f_{i,2}}{f_{i,1}} = K; \quad \mu_i^\circ = \mu \text{ of pure component}$$

where K is the distribution coefficient, cannot be expected to be constant except over small increments of Δx_1 even though it is often considered so in describing extraction processes. In the diagram $[(bd/bc) > (eg/ef)]$ even dilute solutions diverge rapidly from ideal behavior. Figure 2 shows an example where at solute levels as low as 1% stating solute levels does not uniquely define K_{D_1} :

$$(6a) \quad K_{D_1} = [i,2]/[i,1]$$

in a ternary system where methyl oleate is distributed between hexane and acetonitrile.²⁶ Two of the three component percentages must be specified to fix K_{D_1} . Therefore, more complete equilibrium data are needed to accurately predict and evaluate separation parameters.

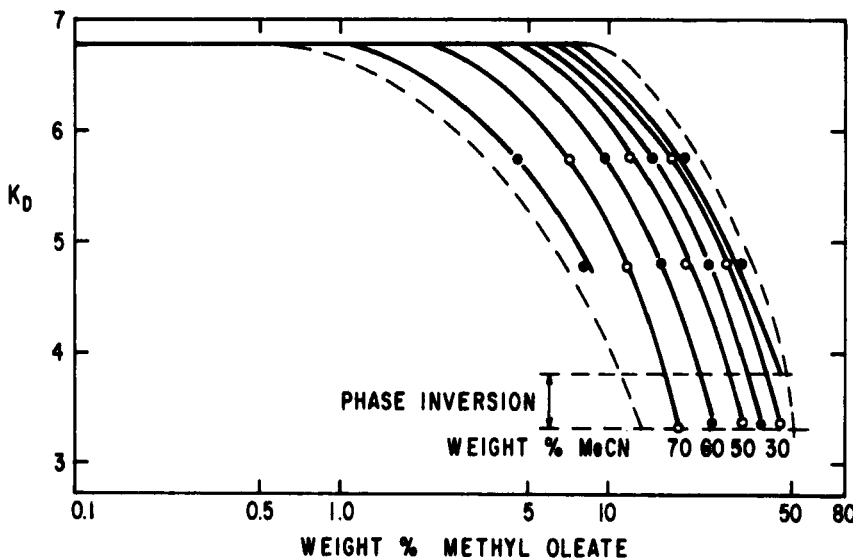


FIGURE 2

Partition coefficient as a function of methyl oleate and acetonitrile concentration at 30.4°C. Hexane is third component.
 K_{D_1} = molar conc. oleate in hexane-rich layer/molar conc. in acetonitrile-rich layer

Equilibrium relationships in a quaternary system are depicted in Figure 3. Figure 4 shows three of the faces of the quaternary diagram and a ternary representing a plane of constant solvent ratio cutting the solid which defines the region of immiscibility. Hexane, methyl 9-octadecenoate (MeO) and methyl 12,13-epoxy-9-octadecenoate (MeV) are miscible in all proportions at 25°C. Ter-

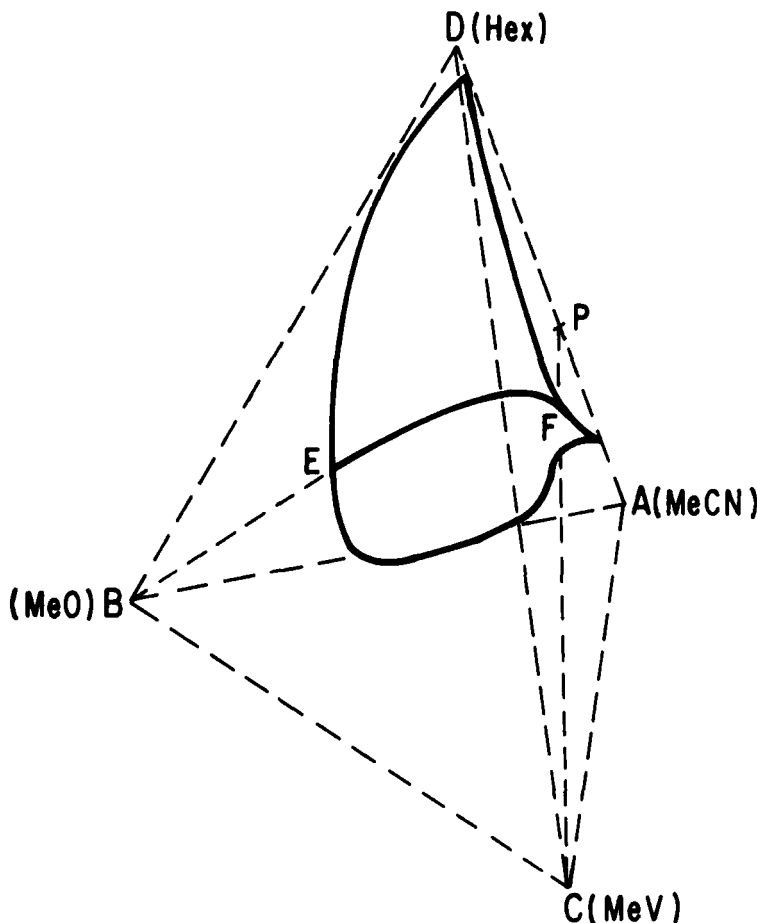


FIGURE 3

Schematic drawing of quaternary diagram at 25°C.
 A. acetonitrile (MeCN) B. methyl 9-octadecenoate (MeO)
 C. methyl 12,13-epoxy-9-octadecenoate (MeV) D. hexane (Hex)

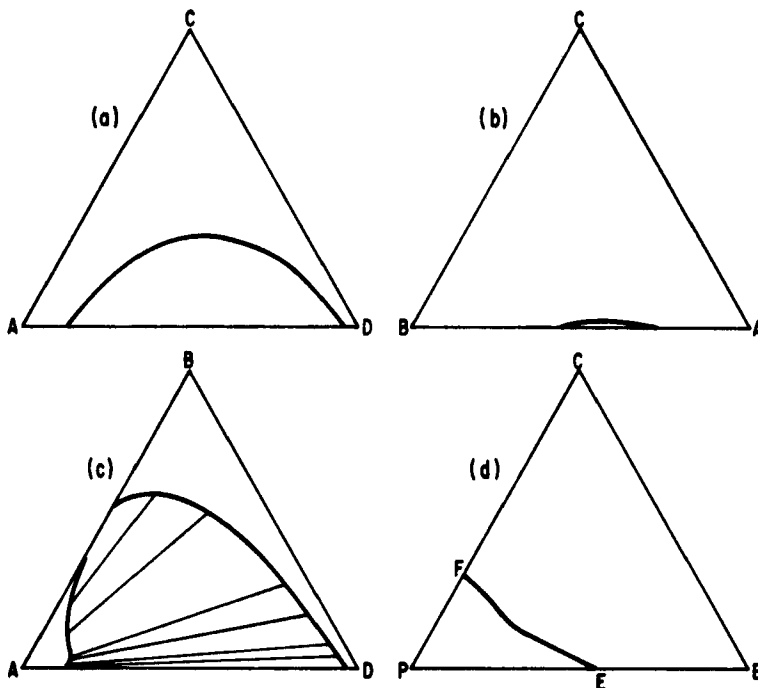


FIGURE 4
Three faces of quaternary diagram. A, B, C, D as in Figure 3. (d) CBE plane, P = 60% Hex, 40% MeCN

nary and quaternary solubility data is given in Tables I and II. Since MeO is less soluble in MeCN than MeV (ternary ABC) a possible separation of the two using a hexane-acetonitrile solvent system was suggested. Examination of equilibrium data (Table III) confirmed the greater selectivity of MeCN for the MeV over most of the useful region of the system.

These data also show that at high solute levels it would be possible for the system to move from a two- to a useless one-phase system as purification of MeV progressed. Furthermore, there exists a line (isopycnic) on the MeO face above which the Hex-rich phase becomes the denser phase while no such line occurs on the MeV

TABLE I
Ternary Solubility Data (Weight %)

<u>Methyl Oleate</u>	<u>Methyl Vernolate</u>	<u>Acetonitrile</u>	<u>Hexane</u>
-	-	85.5	14.5
6.6	-	79.9	13.5
11.3	-	80.1	8.6
11.7	-	80.3	8.0
17.8	-	77.0	5.2
21.2	-	75.6	3.3
28.3	-	70.4	1.3
28.6	-	71.4	-
-	-	4.2	95.8
38.2	-	11.8	50.0
48.1	-	15.2	36.7
58.1	-	32.7	9.2
55.8	-	44.2	-
-	10.0	7.4	82.6
-	22.3	10.9	66.8
-	9.3	74.6	16.1
-	23.1	55.0	21.9
-	28.4	25.4	46.2
-	24.2	13.4	62.4
-	30.8	35.0	34.2
-	10.5	73.7	15.8
-	2.7	3.7	93.6
-	6.2	79.3	14.5
-	16.9	63.7	19.4
-	12.2	16.5	81.3
54.0	1.2	44.8	-
45.2	1.6	53.2	-

TABLE II
Quaternary Solubility Data at 25°C (Weight %)

<u>Methyl Vernolate</u>	<u>Methyl Oleate</u>	<u>Acetonitrile</u>	<u>Hexane</u>
9.2 ^a	4.9	6.3	79.6
8.3 ^a	4.5	72.6	14.6
15.7 ^a	8.5	55.9	19.9
5.0 ^b	9.2	5.7	80.1
4.7 ^b	8.6	74.6	12.1
8.9 ^b	16.5	60.1	14.5
13.3 ^b	24.6	37.8	24.3

^a 65 MeV/35 MeO

^b 35 MeV/65 MeO

TABLE III
Tie Line Data
(25 °C)

Hexane-Rich Phase						Acetonitrile-Rich Phase					
Methyl Vernolate	Methyl Oleate	Aceto- nitrile	Hexane	Density g/ml		Methyl Vernolate	Methyl Oleate	Aceto- nitrile	Hexane	Density g/ml	Mass Ratio
-	20.9	6.8	72.3	0.700	-	2.8	82.7	14.5	0.756		
-	34.3	9.1	56.6	0.727	-	5.0	80.9	14.1	0.762		
-	51.6	18.9	29.5	0.794	-	11.1	79.7	9.2	0.776		
-	58.5	31.2	10.3	0.809	-	21.1	75.9	3.0	0.786		
2.5	-	4.5	93.0	0.669	2.6	-	83.2	14.2	0.758		
5.0	-	4.9	90.1	0.679	4.8	-	80.9	14.3	0.766		
9.7	-	6.1	84.2	0.691	9.3	-	75.2	15.5	0.771		
15.7	-	8.3	76.0	0.705	15.0	-	67.5	17.5	0.775		
21.1	-	10.9	68.0	0.718	20.1	-	59.7	20.2	0.780		
23.9	-	12.3	63.8	0.723	24.1	-	53.0	22.9	0.772		
2.8 ^a	9.1	5.0	83.1	0.688	2.4	1.2	82.1	14.3	0.764	1.33	1.40
1.4 ^a	5.0	5.2	88.4	0.677	1.4	0.6	84.8	13.2	0.761	1.40	1.40
5.5 ^a	15.8	6.7	72.0	0.708	4.4	2.3	79.6	13.7	0.766	1.19	1.18
8.8 ^a	22.6	10.6	58.0	0.731	6.5	4.0	75.7	13.8	0.767	1.05	1.05
11.6 ^a	26.5	16.9	45.0	0.749	8.3	5.9	72.0	13.8	0.774	1.37	1.55
1.0 ^b	1.1	4.6	93.3	0.670	1.0	0.1	84.7	14.0	0.761	1.45	1.40
5.0 ^b	5.1	4.6	85.3	0.685	4.6	0.7	80.7	13.8	0.764	1.42	1.44
15.5 ^b	12.7	10.0	61.8	0.726	12.8	3.0	68.4	15.8	0.771	1.21	1.21
20.7 ^b	14.3	19.3	45.7	0.749	16.6	5.1	59.8	18.5	0.776	1.01	1.11

^a 35 MeV/65 MeO

^b 65 MeV/35 MeO

^c Eq. (7)

face. Although no attempt was made to define it experimentally, an isopycnic surface must cut the face ABD and the immiscibility surface between the ABD and ACD faces. Besides the obvious difficulties that would result from phase inversion during a fractionation, severe lengthening of phase settling times were observed as the isopycnic line was approached. Imperfect transfers would result.

Equation (3) indicates the temperature dependence of K_1 while Figure 5 depicts a significant contraction of the immiscibility region over only a ten degree change. The K_D , at constant B and A/D, varied by about 29% over the range. A 12% decrease in K_{D_2}/K_{D_1} was observed when the temperature of a similar system²⁶ was increased from 20 to 30°C. Wankat²⁷ has exploited such variations in a multiple solute input process by alternating temperature between two values in a stepwise manner and evaluated the application of this approach to preparative separations. Generally, however, temperature is selected prudently to enhance solute selectivity of the system and extractions performed isothermally.

A temperature exists above which MeO and MeCN (Figure 5) are completely miscible (Critical Solution Temperature). The region defined by the dashed line was not accurately determined. The MeO-MeCN-Hex (30°C) and the MeV-MeCN-Hex systems exhibit "plait points" where the equilibrium "tie" lines merge and the compositions of the phase are identical ($K = 1$). As these critical points are approached small changes in composition or temperature alter the system's properties considerably. In spite of this difficulty, Hollingsworth²⁸ surprisingly demonstrated by theory and experiment that in some cases at low solute levels there is an optimum temperature or solvent composition near a critical point of the solvent system where the maximum separation can be achieved for a given number of extraction cells and transfers. Although pressure is thermodynamically relevant to phase relationships in liquids, its effect can be considered negligible in systems commonly employed in the extraction.²⁹

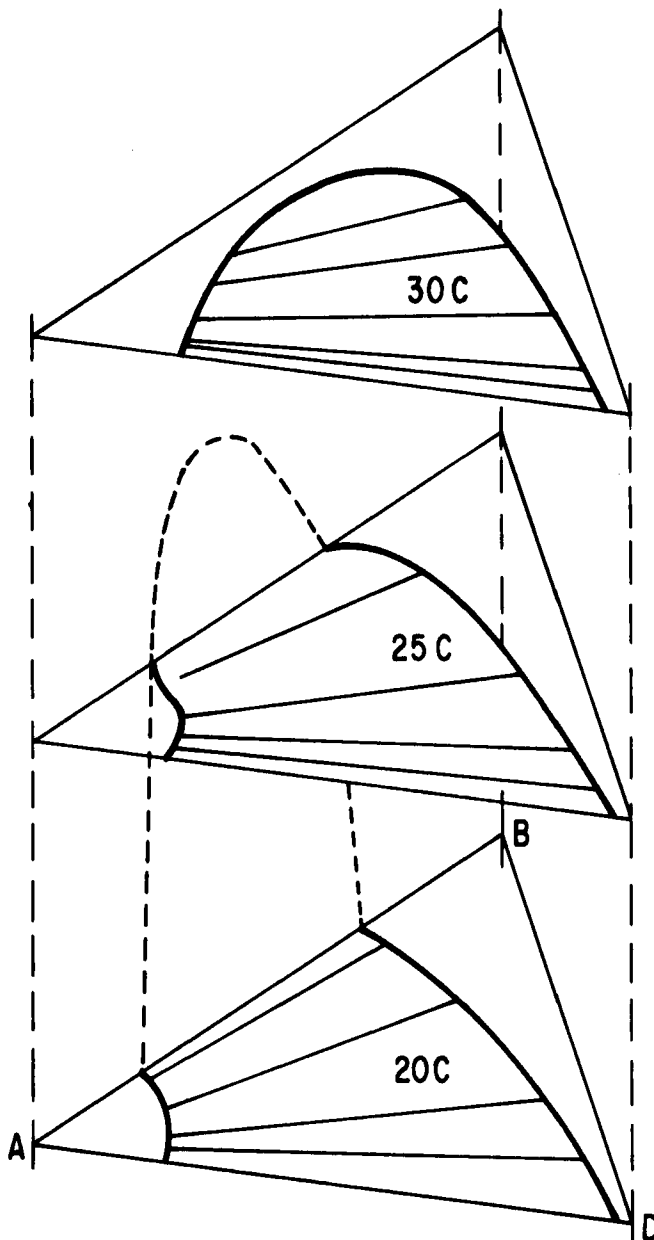


FIGURE 5
Temperature effects on ternary system. ABD as in Figure 3.

As seen in Figure 5, the addition of temperature as a variable complicated the representation of phase relationships. Beyond four variables, simple visual representation in two dimensions becomes virtually impossible. Palatnik and Landau³⁰ have applied the techniques of vector notation, linear algebra, and topology to the description of multi-variable (X_1 , T, P, etc.) systems. Aspects of this approach have been advantageously applied to quaternary systems.³¹ It was shown, for example, that the Lever Rule which Gibbs³² derived for three component systems and triangular coordinates could be generalized for n-components and n-1 dimensions so that for the MeV-MeO-Hex-MeCN 2-phase system:

$$(7) \quad \frac{P_2}{P_1} = \frac{L_1}{L_2} = \frac{w_{i,1} - w_i}{w_i - w_{i,2}}$$

where P_1 and P_2 are masses of phases 1 and 2, L_1 and L_2 are lengths of line segments (hypervolumes) connecting points in space which represent compositions of phases 1 and 2 and the point representing total composition; $w_{i,1}$ and $w_{i,2}$ are the weight fractions of each component. The average L's and the experimentally determined masses lends credibility to the drawn contours of the diagram. A significance of the Lever Rule is that given the phase diagram, the progress of an extraction can be predicted. This will be demonstrated later.

Although the thermodynamic studies are important and useful, a deterrent to their application is the large numbers of Cloud point titrations and tie line determinations that must be made. In some cases, particularly with biochemically important solutes, quantities of pure materials are too limited for such experiments. Francis³³ has made a significant contribution to the literature, graphing over 1,000 ternary systems involving about 300 components.

Albertsson depicted a number of phase diagrams of aqueous-polymer systems such as Dextran-Tergitol-H₂O and Potassium phosphate-poly-ethylene glycol-H₂O.¹⁸ He employed the immiscible regions in these systems for the purification of viruses, enzymes, and microbial cells. Most likely, it is the nature of solvent interactions that

the literature will provide, further experimentation being required to completely define the system with particular solutes.

It would be advantageous to obtain the most information about an extraction system with the minimum number of experiments. A number of empirical or semi-empirical approaches have been proposed^{34,35,36,37} which are solutions to the integrations of the Gibbs-Duhem equation (eq. (5)).

One commonly used solution for ternary systems^{29,34} is given below:

$$(8) \quad \log f_i =$$

$$\frac{x_j^2 I_{ij} \left(\frac{I_{ji}}{I_{ij}} \right)^2 + x_k^2 I_{ik} \left(\frac{I_{ki}}{I_{ik}} \right)^2 + x_j x_k \left(\frac{I_{ji}}{I_{ij}} \right) \left(\frac{I_{ki}}{I_{ik}} \right) I_{ij} + I_{ik} - I_{kj} \left(\frac{I_{ik}}{I_{ki}} \right)}{x_i + x_j \left(\frac{I_{ji}}{I_{ij}} \right) + x_k \left(\frac{I_{ki}}{I_{ik}} \right)}$$

where I_{ij} , etc., are empirical functions which describe the interactions of groups of dissimilar molecules. They may be determined from mutual solubilities of the three binary pairs; for example:

$$(9) \quad I_{ij} = \frac{\log \frac{x_{ij}}{x_{ii}}}{\frac{1}{\left(1 + \frac{I_{ij} x_{ii}}{I_{ji} x_{ji}} \right)^2} - \frac{1}{\left(1 + \frac{I_{ij} x_{ij}}{I_{ji} x_{jj}} \right)^2}}$$

$$(10) \quad \frac{I_{ij}}{I_{ji}} = \frac{\left(\frac{x_{ii}}{x_{ji}} + \frac{x_{ij}}{x_{jj}} \right) \left(\frac{\log \frac{x_{ij}}{x_{ii}}}{\log \frac{x_{ji}}{x_{jj}}} - 2 \right)}{\frac{x_{ii}}{x_{ji}} \frac{x_{ij}}{x_{jj}} - \frac{2x_{ii} x_{ij}}{x_{ji} x_{jj}} \frac{\log \frac{x_{ij}}{x_{ii}}}{\log \frac{x_{ji}}{x_{jj}}}}$$

where x_{ii} is the fraction of i in the i -rich phase, etc. Plots of solute activity vs. fraction of solute are constructed by combining the calculated solute activity coefficient with experimentally determined solubility curves and the equilibrium compositions obtained. Wohl³⁴ evaluated this approach and found it restricted in its applicability.

Other approaches have included expressions which took into account local composition variations in liquid mixtures which resulted from interactions between molecules.

Wilson³⁵ based an equation on the Flory-Huggins concept which related G^E to the differences in the molecular sizes of solution components, but in the proposed equation, "local volume fractions" were introduced to account for nonrandomness. Each "local volume" fraction was calculated from an expression containing an adjustable parameter (interaction energy) obtained from some experimental points.

Heil³⁶ extended this approach and added additional interaction terms but still used two adjustable parameters per binary.

Renon³⁷ developed an equation (NRTL) assuming that a binary solution is composed of two kinds of cells each with a different component at the center and that the composition of these cells is related to the interaction energy between the components, which is described by three adjustable parameters. The Gibbs excess energy results from the transfer of molecules of each component from cells of pure component to cells of solution. All three approaches may be expressed in the general equation:³⁸

$$(11) \quad \ln f_i = \zeta \left(1 - \ln \sum_{j=1}^{\#} x_j s_{ji} - \sum_{j=1}^{\#} \frac{x_j s_{ij}}{\sum_{k=1}^{\#} s_{kj} x_k} \right. \\ \left. + \phi \left[\frac{\sum_{j=1}^{\#} \tau_{ji} s_{ji} x_j}{\sum_{k=1}^{\#} s_{ki} x_k} + \sum_{j=1}^{\#} \frac{x_j s_{ij}}{\sum_{k=1}^{\#} s_{kj} x_k} \left(\tau_{ij} - \frac{\sum_{\ell=1}^{\#} x_{\ell} \tau_{\ell j} s_{\ell j}}{\sum_{k=1}^{\#} s_{kj} x_k} \right) \right] \right)$$

where $s_{ji} = \rho_{ji} \exp(-\alpha_{ji} \tau_{ji})$

$$\tau_{ji} = (g_{ji} - g_{ii})/RT$$

Tau and alpha are the adjustable parameters; $\alpha = 1$ in Wilson and Heil equations; ρ_{ji} the molar volume ratio of a component pair, $\rho = 1$ in NRTL equation; $\zeta = 0$ in NRTL, 1 in others; and $\varphi = 0$ in Wilson, 1 in others. Since only component pairs are considered, theoretically the equation is general for any number of components.

Binary parameters should be computed from vapor-liquid equilibrium measurements using curve fitting techniques,³⁹ but for best results some tie line data were used to calculate the binary parameters. A typical comparison for a ternary system is shown in Figure 6.³⁷ While the agreement between the NRTL, Heil, and experiment in this case is good, it is doubtful whether the predicted equilibrium could be used to describe an extraction precisely. Some good correlations of four component vapor-liquid equilibrium data³⁹ using binary parameters and the Wilson equation have been reported, but this equation cannot predict phase immiscibility, and so it has little relevance to liquid extraction. No correlations for liquid-liquid systems with more than three components seem to have been reported using the other equations. The problem remains, then, to predict in detail the systems of two or more solvents and several solutes, the kind which are generally encountered in discontinuous liquid extraction. Nevertheless, some useful information about single solute-solvent interactions can be obtained and K or K_D estimated. In some cases, however, the complete equilibria need to be considered especially at high solute levels³¹ to evaluate separations parameters.

The "regular solution" theory of Hildebrand and Scott²⁵ is also used as a basis for approximating selectivities. According to this model if the energy of two molecules depends only on the distance between them (London forces), no specific interactions such as dipole interactions of hydrogen bonding exist, the molecules are randomly distributed, and there is no volume change on mixing at constant pressure:

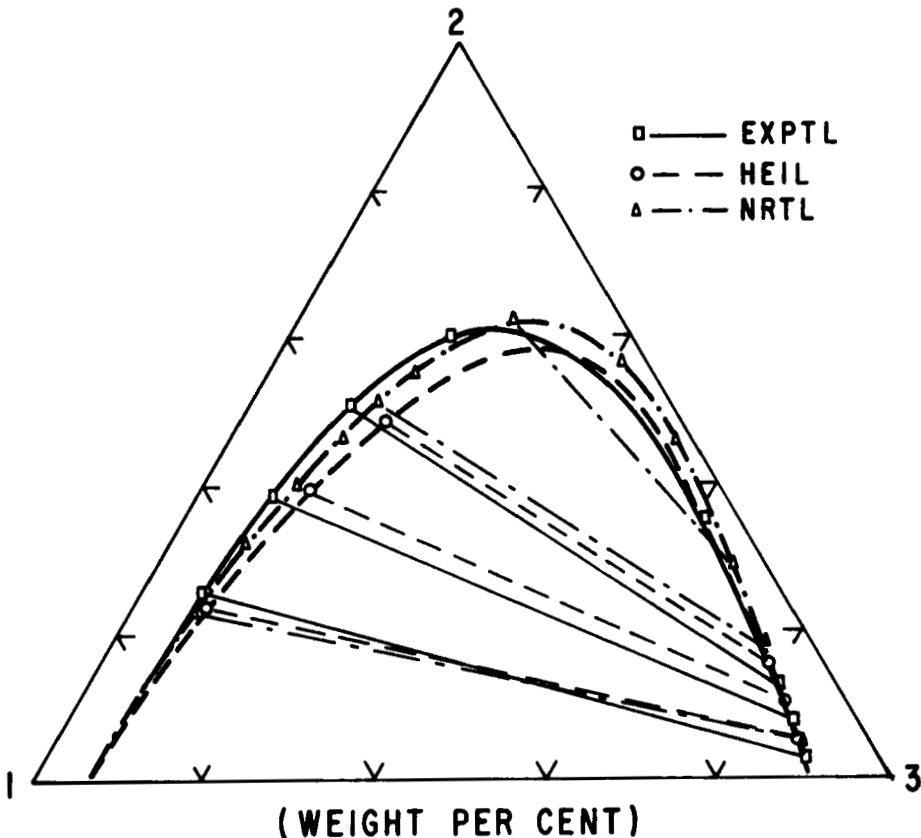


FIGURE 6
 Calculated and observed liquid-liquid equilibria at 0 C.³⁷
 Reproduced by permission A.I.Ch.E.

$$(12) \quad RT \ln f_1 = v_1 \phi_2^2 (\sigma_1 - \sigma_2)^2$$

where V_1 = molar volume of component 1, ϕ_2 = volume of fraction of component 2 in solution and σ_1 and σ_2 are the solubility parameters of 1 and 2. The solubility parameters are defined as

$$(13) \quad \sigma = \left(\frac{\Delta H_v - RT}{V} \right)^{\frac{1}{2}}$$

and results from the statistical thermodynamic⁴¹ approach to the estimation of energy of mixing. Compilations of solubility parameters of common organic compounds exist^{25,31,42,43} and Hoy⁴³ has calculated group contributions to the solubility parameter for a number of functional groups so that Small's approach⁴⁴ for predicting the solubility parameter from knowledge of structure could be applied to most organic compounds. It would seem, then, that K or K_2/K_1 could be calculated from eq. (12) and eq. (6):

$$(14) \quad RT \ln K_2/K_1 = v_1 [(\sigma_1 - \sigma_U)^2 - (\sigma_1 - \sigma_L)^2] + \\ v_2 [(\sigma_2 - \sigma_U)^2 - (\sigma_2 - \sigma_L)^2] .$$

In most cases, however, this is only an approximation to K because: the assumptions leading to eq. (13) are usually not valid in terms employed in extraction even when a nonideal entropy term, etc. (15)⁴⁵, is added:

$$(15) \quad \ln K_2/K_1 = (v_2 - v_1) \left(\frac{1}{v_L} - \frac{1}{v_U} \right) + \\ \frac{2v_1}{R_T} (\sigma_U - \sigma_L) (\sigma_U - \sigma_L)$$

and because the nature of the equation magnifies errors in σ . Furthermore, as noted earlier K is rarely constant and its infinitely dilute value has limited utility. K ratios at infinite dilution were 17, 13, and 8 (for the MeO-MeV-Hex-MeCN system described earlier) as obtained by eq. (14), eq. (15), and experiment. Considering the assumptions, the agreement in ratio is good in this case. However, when the individual K's were calculated, extremely wide divergence from experimental values was observed. Irving⁴⁶ has surveyed in depth the application of the solubility parameter concept to extraction. He found Scott's⁴⁷ earlier comment about the concept still appropriate: "In short, the solubility parameter equations offer a useful approach to a very wide area of solutions, like a small-scale map for a very broad long-distance air view of a subcontinent. It is able to make numerical predictions about all

areas; these are unlikely to prove highly accurate when a small area is examined carefully, but they are equally unlikely to prove completely absurd."

Davis⁴⁸ has reviewed the group contribution approach to solution thermodynamics and contributed new developments in this area.⁴⁹ Harris⁵⁰ has reported better correlations using molar surface area of the groups instead of volumes. Hopefully, current research in the structure of liquids and interactions of their mixtures will soon provide more useful models for predicting separation systems.

In the previous discussions only single species were considered. Frequently, solutes are present in more than one form. They may be dissociating acids or bases or complexed metals. In such cases, acid or base dissociation constants and/or stability constants of the complexes must be included in the overall distribution coefficient, which reflects then a dependence on pH and/or ligand concentration (Figure 7 and eq. (16)). These complex equilibria must be studied individually to evaluate manipulable separation parameters and a number of these, as well as equilibria involving liquid ion-exchangers,^{5,19,51,52,53,54} have been reported.

$$(16) \quad D_C = [CA]_2 \beta_C / [C^{z+}]_1 = K_D K_{eq} K_a^z [HA]_2 \beta_C / K_A^z [H^+]^z$$

Scholfield and coworkers⁵⁵ have made splendid use of the ability of Ag^+ to form pi-complexes with double bonds to achieve separations of fatty acid methyl esters, including cis-trans isomers, and triglycerides.

Albertsson¹⁸ has described equilibria in which adsorption at the liquid-liquid interface influenced separation of macromolecules and cell particles. He showed that for spherical particles

$$(17) \quad K = e^{-\frac{4\pi r^2 (\gamma_{1,U} - \gamma_{1,L})}{kT}}$$

where $\gamma_{1,U}$ is the interfacial tension between the particle and the upper phase and r is the particle radius. If the macromolecules

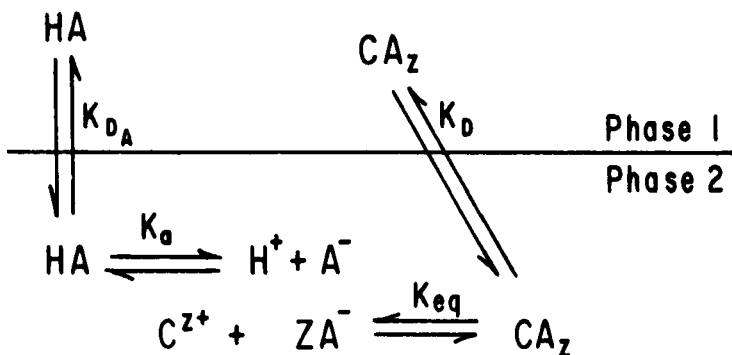


FIGURE 7
Example of distribution with multi-equilibria

are polyelectrolytes, the equilibrium was described in terms of the Donnan potential. In the presence of excess salt (AB):

$$(18) \quad \ln K'_z = \ln K_z + \frac{Z}{2} \ln \frac{K_A^+}{K_B^-}$$

where K' and K^+ are the distribution coefficients in the presence and absence of the electrical potential respectively. Separations can be influenced by the nature of the salt.

In addition to selectivity, solvents for liquid-liquid extraction should have great density differences, high interfacial tension of the phases, and low viscosities; all of these properties are a result of mass transfer and phase settling considerations. Flammability, toxicity, and corrosiveness also need to be evaluated as does cost.

PROCEDURES

Having found a potentially useful solvent system, the fractionation is carried out, generally in a robot controlled device in which large numbers of distributions and transfers can be made. Basic descriptions of such devices have been referred to in the introduction. Suppliers of automated instruments can be found in resources such as Science's Annual Guide to Scientific Instruments

and Analytical Chemistry's Labguide. They are listed as "countercurrent distributors," the name coined by the late Dr. Lyman C. Craig,^{56,57,58} who developed much of the early theory, described the first distributors, and demonstrated the utility of the approach to complex separations problems. While the distributors vary mechanically as to how equilibration, settling, and transfer is achieved, they can be viewed schematically as in Figure 8. Mixing takes place in part I, and after settling all liquid (mostly upper layer, V_U) above a side arm (C.P.) is transferred to part II. Subsequently the liquid in II is transferred to next tube and another cycle begun. In some devices^{14,15} the other layer (V_L) is also transferred; in others the equilibration chambers are separated by spacers containing eccentrically placed holes so that as the device rotates upper phase transfers when the hole reaches its lowest position. In any case, because of variation in phase volumes as solute concentration changes, V_L may become smaller and not reach C.P. causing some V_U to be retained (V_{UR}) during transfer. In some distributors,

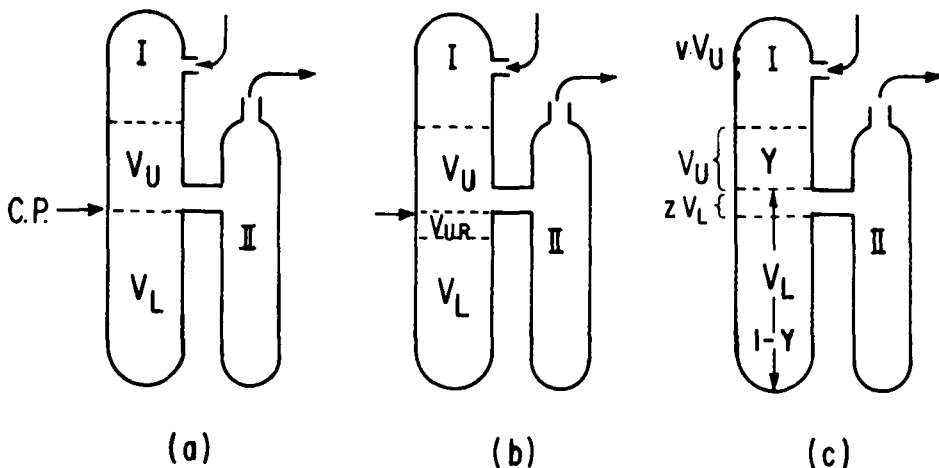


FIGURE 8
Schematic of distribution tube showing perfect (a)
and anomalous transfer effects

lower phase is added on each cycle to make up for decreased V_L so that a portion of V_L is transferred. Also, some V_U (vV_U) may be retained on walls of I, altering the supposed V_U/V_L ratio (Figure 8c). Consider a series of tubes which had been filled with upper and lower phase and into tube "0" solute is introduced while zV_L ml of lower is added as makeup. After equilibration (Fig. 8c), let Y = fraction of solute distributed in upper phase, then $(Y + z(1 - Y) - vY) =$ the fraction of solute to be transported to tube 1. Let A be the fraction remaining so that $vY + (1 - Y) - z(1 - Y) = A$. The process is contained in Figure 9 where examination of the coefficients shows the development of a distribution of the form:

$$(17) \quad (A + (1 - A))^N$$

which is the binomial distribution.

Therefore, from the properties of the binomial, expressions for the total amount of solute (Q) in tube M (eq. (18)), the position of the distribution maximum (eq. (19)), and its standard deviation, Σ , (eq. (20)) may be written for any number of transfers, N :

$$(18) \quad Q_{N,M} = \frac{N!}{M! (N-M)!} (1 - A)^M (A)^{N-M}$$

$$(19) \quad M_{\max} = N(1 - A)$$

$$(20) \quad \Sigma = \sqrt{N(1 - A)(A)} = \sqrt{\frac{M_{\max}}{N} A}$$

From eq. (6a):

$$K_{D_i} = (Y/V_U) / (1 - Y/V_L) = YV_L / V_U - V_U Y$$

so that

$$(21) \quad Y = (K_{D_i} s) / ((K_{D_i} s) + 1)$$

where $s = V_U/V_L$.

If it is assumed that K_{D_i} , v , and z are constant, the distribution profile of a solute mixture can be calculated. This pro-

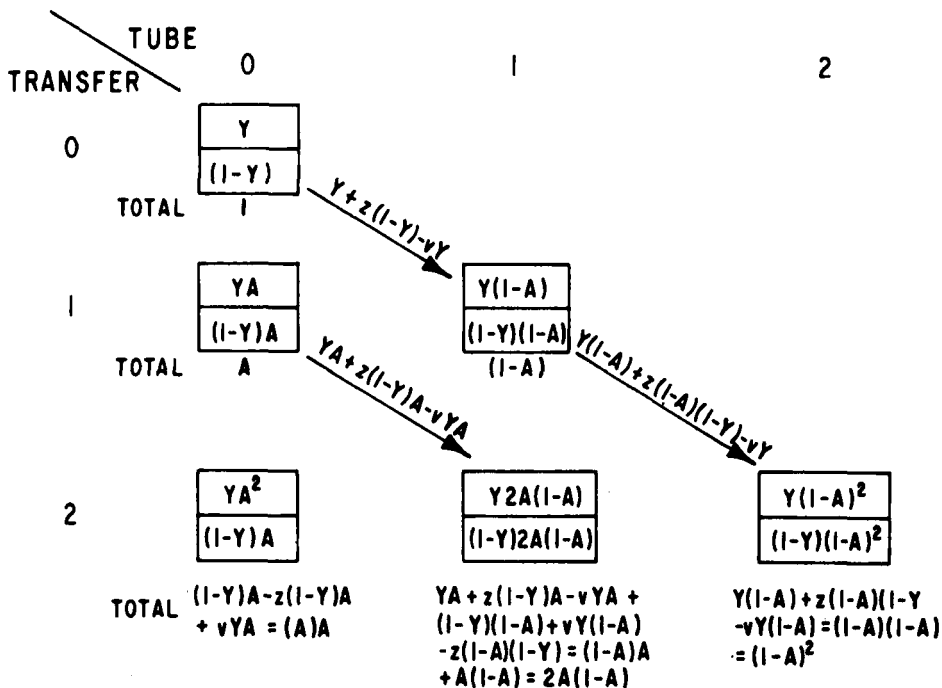


FIGURE 9
Distribution Scheme

cedure where all solute remains in the distributor is often called the "fundamental" method. An example of an application of this method for the comparison of liver lipids from a control rat and a rat exposed to severe cold⁵⁹ is given in Figure 10. When $v = 0$ and $z = 0$, the commonly used ideal equations⁵⁷ result. Later discussion will demonstrate, however, the necessity of considering two-phase flow.

If $z = 0$ and V_L does not reach C.P. (Figure 8) and $(1 - Y)$ is defined as the fraction of solute adsorbed at the solvent interface, these equations may also be used to describe interfacial countercurrent distribution¹⁸ even though the mechanism of interaction is different.

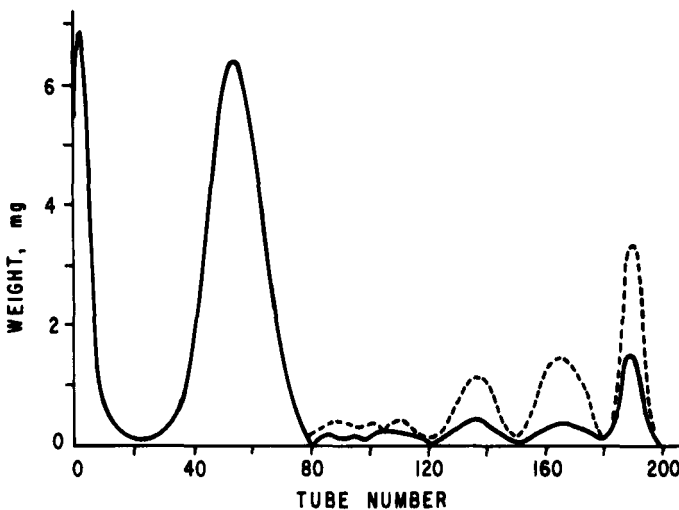


FIGURE 10

Distribution of Rat Tissue Lipids ⁵⁹

(—) control (—) exposed to severe cold.
 Tubes 0-80, phospholipids; 80-120 free fatty acids,
 120-150 free cholesterol; 150-180 diglycerides;
 180-200 triglycerides and cholesterol esters.

Reproduced by permission from National Research Council of Canada

When enough transfers are made, M_{\max} will be the last tube (M'_{\max}) and one more transfer will elute solute from the distributor. Hence, c , the number of tubes or cells in the distributor (number of first tube = 0) is from eq. (19)

$$(22) \quad c = M'_{\max} + 1 - N_{\max} (1 - A) + 1$$

and N_R , the number of transfers required to elute peak:

$$(23) \quad N_R = N_{\max} + 1 = \text{but } N_{\max} \gg 1$$

so that

$$(24) \quad N_R = (c - 1)(1 - A)$$

and the fraction of solute in N_R is that in the upper phase at $(N_R - 1)$ transfers. Evaluating the stepwise process as was performed for the fundamental distribution, another binomial distribution

was obtained to describe the elution profile or single withdrawal procedure.

$$(25) \quad F_N = \frac{N!}{c!(N-c)!} (1-A)^c (A)^{N-c}$$

Gaussian approximations to the binomial have been employed to simplify calculations^{57,60} and to permit use of tables of the normal curve.

$$(26) \quad Q_{N,M} = \frac{1}{\sqrt{2\pi M}} \exp - \left(\frac{(M_{\max} - M)^2}{2M} \right)$$

$$(27) \quad F_N = \frac{1}{N_R} \left(\frac{c}{2\pi A} \right)^{\frac{1}{2}} \exp - \left(\frac{(1-A)^2}{2Ac} (N - N_R)^2 \right)$$

With these expressions the progression of a separation can be approximated. Equations (19) and (20) show that, for a given solute, width of a band inside the distributor increases with the square root of the number of transfers. For a series of solutes, since $((A)(1-A))^{\frac{1}{2}}$ in practical systems (.9 > A > .1) are similar, the widths are similar after a given number of transfers. Theoretically each tube contains solute so that width is taken as some multiple of Σ , for example $\pm 2.33 \Sigma$ indicates that 99% of the solute is included in the measurement. The Gaussian approximation suggests that width is a function of the position of the band in the distributor ($\Sigma = \sqrt{M}$) so that each band as it progresses through will have the same width as it reaches a given position in the distributor. Examination of eq. (20) shows that this is a reasonable approximation. To reach a given M_{\max} , the product $N(1-A)$ will be constant, so that Σ varies only with $(A)^{\frac{1}{2}}$. For most cases, ratios of $(A)^{\frac{1}{2}}$ for the first and last peaks will be close to one. However, widths after application of enough transfers to elute all solutes will differ considerably. The results of a simulated distribution are given in Table IV to illustrate these effects.

Figure 11⁶⁰ compares an experimental elution where two-phase flow occurred with profiles calculated using equation (27) and the

TABLE IV

K_D	$(1-A)$	<u>72 TRANS</u>		<u>91 TRANS</u>		<u>245 TRANS</u>		<u>ELUTION</u>	
		M_{max}	Σ	M_{max}	Σ	M_{max}	Σ	N_R	Σ
1.20	.545	39	4.3	-	-	-	-	112	8.7
.75	.428	31	4.2	39	4.7	-	-	147	12.4
.19	.158	11	3.1	14	3.5	39	5.7	420	41.1

commonly used ideal expression ($v = 0$, $z = 0$). In this case two-phase flow had no influence on the middle peak but the earliest peak eluted later than predicted by the ideal equation while the last peak eluted earlier than predicted. The detrimental effect of this peak shifting due to imperfect transfers and use of co-current is obvious. The modified equations approximated the experimental peaks more closely, although even at the low solute levels used z and v could not be maintained constant.

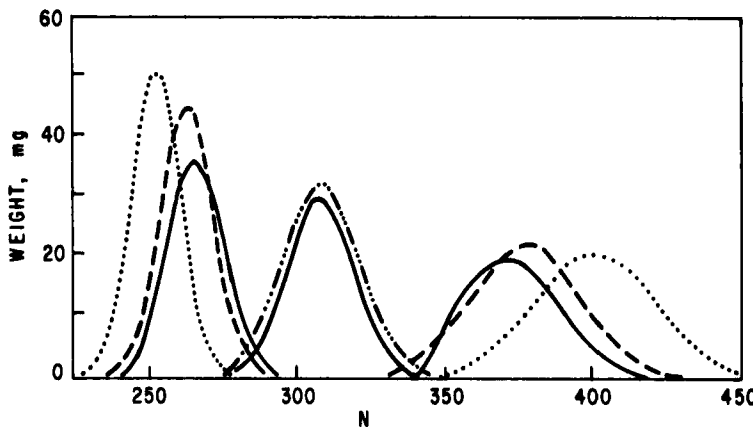


FIGURE 11

Comparison of experiment and theory.

(—) exp, (· · · ·) ideal equation $z = 0$, $v = 0$; (---) eq. (27) $z = .14$, $v = .08$. $c = 200$ $K_{D1} = 16.1$, $K_{D2} = 7.8$, $K_{D3} = 4.2$.

In practice, it is generally desirable to fractionate larger amounts of solute than can be introduced in a single input. One method of increasing the amount distributed and at the same time minimizing volume reorganization effects, involves addition of solute incrementally to the zeroeth tube. If K_D , z , and v are considered constant, a parade of identical profiles, each one transfer out of phase with the one preceding it, moves through the distributor. The amount of solute in a tube M , then is the sum of the contributions from each of these out-of-phase profiles or the sum of all the apoints on the leading profile from M to $(M - k)$ for k inputs. If the integral is used to approximate this summation and the Gaussian used to describe the elution or single withdrawal profiles, the following equation results:⁶¹

$$(28) \quad F_{N,k} = \operatorname{erf} \left[\frac{N - N_{Ro}}{\Sigma_o} \right] - \operatorname{erf} \left[\frac{(N - k) - N_{Ro}}{\Sigma_o} \right]$$

where N_{Ro} and Σ_o are the peak location and standard deviation of the single input profiles. For elution profiles:

$$(29) \quad \Sigma_o = (cA)^{\frac{1}{2}} / (1 - A) .$$

In this form of the error function $t = (N - N_{Ro}) / \Sigma_o$. Therefore the distribution with multi-inputs can be calculated using known parameters and tables of Gaussian statistics. Alternatively, the Σ_o obtained from a single input can be employed to "scale up" the amount fractionated. Graphical methods are also used to evaluate the integrals from a plot of the single input distribution or, more conveniently, read from frontal profiles (Figure 12).

Differentiating eq. (28) and setting the derivative equal to zero a description of the effect of multiple inputs on peak maxima is obtained

$$(30) \quad N_R = N_{Ro} + k/2 .$$

Substitution of eq. (30) into eq. (28) leads to:

$$(31) \quad F_{\max} = 2 [\operatorname{erf} (k/2 \Sigma_o)] - 1 .$$

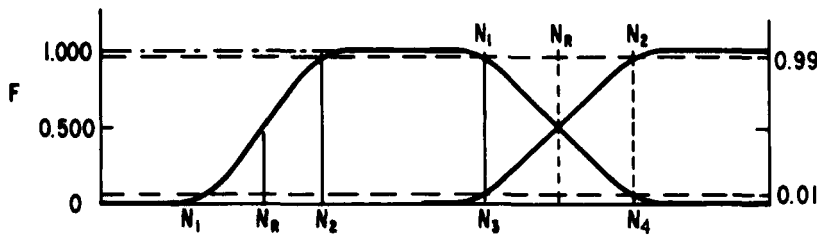


FIGURE 12
Frontal Output Profile

The error function has the property, however, that F approaches one as k becomes very large. Therefore as the number of inputs increases a steady state condition is reached where the amount of solute being fed equals that being eluted when the volume being transferred is constant throughout the distribution. The output profile is a step function which is often referred to as a frontal or breakthrough profile. Once the maximum value is reached additional solute additions will increase the width of the plateau and N_R would have little significance. A new quantity, N_{RF} , is defined which denotes the position of the half height as in the usual procedures or operation, the solute level eventually decreases and in ideal or near-ideal systems, a trailing edge is observed which mirrors the leading edge. The latter is described by the expression⁶⁰

$$(32) \quad F = \sqrt{\frac{(1 - A)^2}{2\pi c A}} \int_{N=0}^N \exp - \left[\frac{(1 - A)^2}{2 A c} (N - N_{RF})^2 \right] dN .$$

Also from the figure:

$$N_1 = N_{RF} + t \Sigma o$$

$$N_2 = N_{RF} + t \Sigma o$$

and since $t_2 = -t_1$, N_F the number of inputs required to produce a step function is

(33) $N_F = 4.66 \Sigma o$,
where the plateau is just reached at $F = 0.99$.

An application of the frontal approach is given in Figure 13 where over 100 g of solute was fractionated.⁶² When large amounts are distributed the ideal or modified ideal equations no longer describe experimental conditions and computer simulations are required. Williams⁶³ determined the variation of K_D with solute level for certain systems and used the equation which fit the data as a basis for simulations of such distributions. The agreement between found and predicted profiles is shown in Figure 14. This approach describes the dissymmetry fairly well, although not all types of nonideal behavior are considered. Martin⁶⁴ developed programs in which all phase relationships could be included, and Rothbart⁶⁰ demonstrated the utility of the approach in several systems. The relationship between experiment, simulated, and ideal output profiles is demonstrated in Figure 15 for a ternary system.

The computer approach, in which no assumptions concerning the profile shape or position are made, is outlined below:

- (1) Ternary solubility curves were described by equations that were determined by least squares methods using the computer.
- (2) Tie lines were described by their slopes and Y intercepts.
- (3) Initial conditions within the distributor and feed profiles were stated.
- (4) The weight and weight fraction of each component in each tube were determined.
- (5) The point describing the system is located on the ternary diagram, and it was determined whether or not this point lay within the immiscible region and below the isopycnic tie line.
- (6) If this point did not fall on a tie line, a new tie line was found by interpolation.

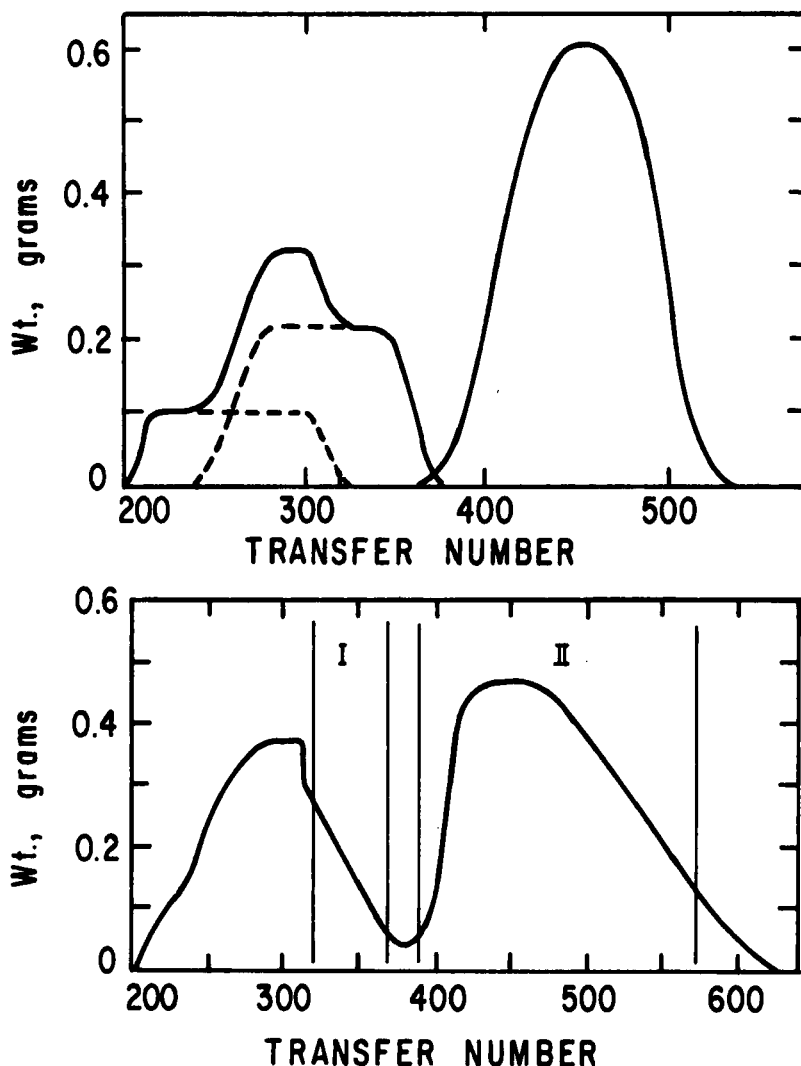


FIGURE 13

Vernonia Oil Fractionation.

- (a) Predicted using eq. (32), ideal form, $V_U = 20 \text{ ml}$, $V_L = 39.2 \text{ ml}$, $c = 200$, 95 inputs - 1 g each.
- (b) Experimental profile 100 inputs, 1.1 g each.
I = divernolin, II = trivernolin, the major projects

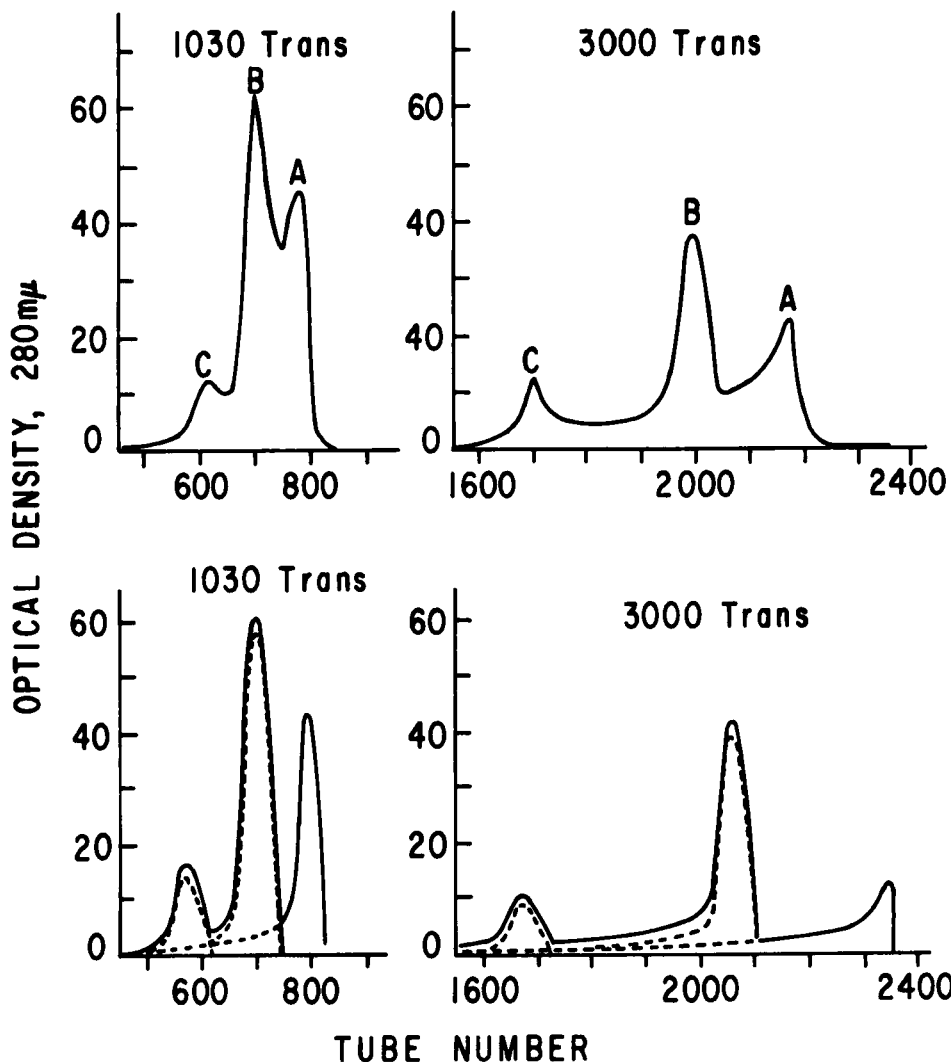


FIGURE 14

Comparison of experimental (upper) and simulated distribution with variable K_D .⁶³ Solutes are tyrocidine C, B, A. Solvents chloroform, methanol. 0.01 N HCl, 2:2:1
 Reproduced by permission of Marcel Dekker, Inc.

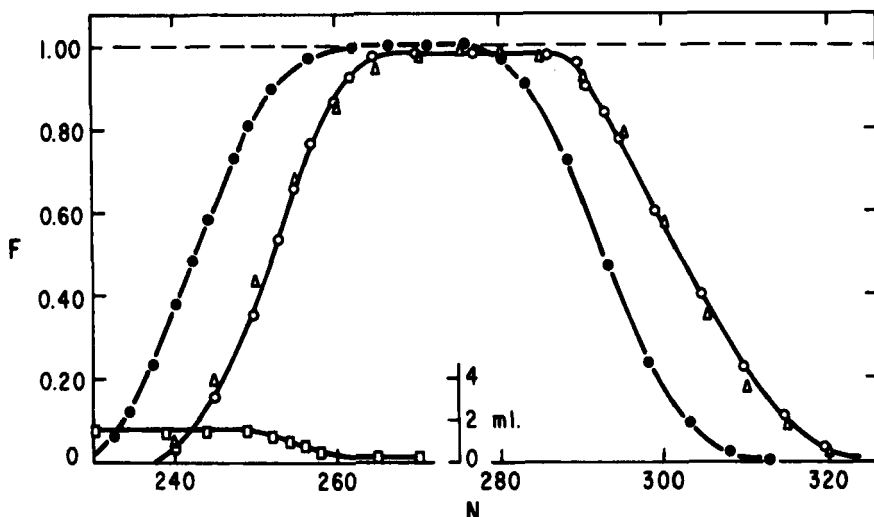


FIGURE 15

Distribution of methyl hexadecanoate in hexane-acetonitrile
 ● output profile calculated from ideal equation.
 $K_D = 8.9$, $V_U = 20$ ml., $V_L = 39.2$ ml.; ○ experimental output;
 △ computer simulated output; □ volume lower phase in output

- (7) The weight fractions of all components in each phase were determined by solving the tie line and solubility curve equations simultaneously, then applying the lever rule.
- (8) Densities, masses, and volume of both phases were determined.
- (9) All material above the cutoff arm, except for a pre-determined amount that was held by the wall, was transferred to the next tube. This process was repeated for as many transfers as were desired.

As seen, the simulation accurately predicts the position, shape, and height of the profile which deviated greatly from that calculated using the ideal equations. Even the pulsing of lower phase as a result of solute dependent volume reorganizations was described. The data demonstrates that, although the common prac-

tice of using solvents pre-equilibrated with each other is worthwhile, it by no means assures constant volume ratio.

Purdy⁶⁵ and Priore⁶⁶ have employed computerized curve fitting methods to analyze experimentally generated profiles in order to estimate purity, even when contaminants were not visually resolved from the major component. Only slight deviations due to volume reorganizations or solute-solute interactions could be handled in these approaches.

Stene⁶⁷ and Craig¹⁴ have demonstrated that the binomial expansion described single input distributions in which upper and lower phases are transferred in opposite directions (CDCD) (Figure 16) when all solute remained inside the distributor, and if no volume reorganizations or transfer effects occurred. As solute emerged, the profile diverged rapidly from the binomial. Alderweireldt¹⁵ extended this rarely used approach by introducing another operating variable, the ratio of upper to lower phase transfers (SSD). By such transfer manipulation, a solute to be purified may be kept near the center of the distributor and contaminants of higher and lower K_D eluted. Day⁶⁸ showed that for the ideal distribution of a single input:

$$(34) \quad F_N = \frac{(N_L + N_U)!}{(N_L + c)!} \left[\begin{matrix} N_L + c & N_U - c \\ Y & (1 - Y) \end{matrix} \right].$$

Stene,⁶⁷ Day,⁶⁸ and Compere⁶⁹ all proposed mathematical treatments of the distribution profiles for single inputs as well as for a large number of inputs. The resulting expressions are very complex and for large numbers of tubes are best solved by computer methods. Their use, therefore, offers little advantage over direct computer simulation. Dutton⁷⁰ has utilized simulation to develop methods for the continuous isolation of pure methylesters from vegetable oil esters.⁷¹ After a large number of inputs are made, a steady-state condition is reached where the amount of solute emerging is constant as inputs are continued. The condition of the distributor at steady-state is shown in Figure 17.⁷⁰ The number of transfers

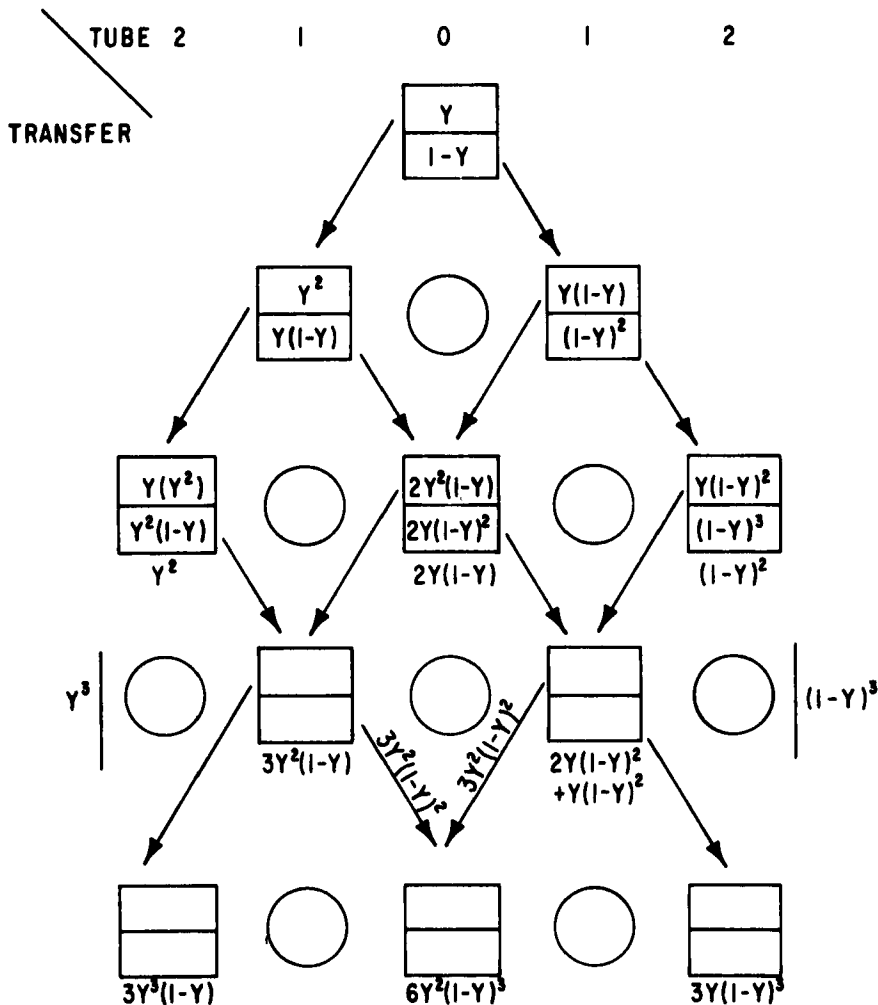


FIGURE 16
Distribution Scheme. CDCD

required to reach steady-state is related to the number of distributor tubes, K_D , the phase volume ratio, and the position of the feed tube. The latter also influences the amount of solute emerging at steady state when the former parameters are constant. For CDCD, the fraction of solute emerging at steady-state is given

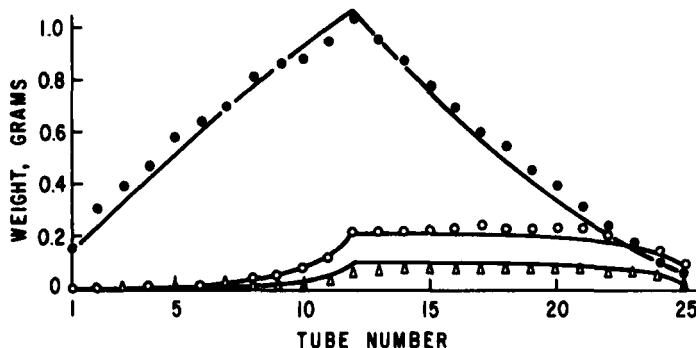


FIGURE 17

CDDC at steady state.⁷⁰
 (—) computer simulation of distribution of corn oil methyl esters; ● exp linoleate, ○ exp oleate, △ exp palmitate. $V_U = 10 \text{ ml}$, $V_L = 50 \text{ ml}$
 Reproduced by permission of Analytical Chemistry

by:⁷²

$$F_{SS} = \frac{\left[(sK_D)^{c_R} - 1 \right] (sK_D)^{c_L}}{(sK_D)^{c_R} (sK_D)^{c_L} - 1}$$

where c_R and c_L are the number of tubes to the right and left of and including the feed tube. In SSD¹⁵

$$(35) \quad F_{SS} = (N_U + N_L) \left(\frac{K_D + 1}{N_U K_D - N_L} \right) .$$

Optimization of Separation

In discussing optimization of separations, a problem of definition is immediately encountered. What is to be optimized - time, quantity of solvent used, amount recovered and purity of all solutes, recovery of one valuable solute at the expense of others, etc.? Much has been written and many concepts⁷³⁻⁸⁰ proposed for the selection of parameters for optimal separation, but still no completely unambiguous definition exists. In preparative separations the experimenter must decide what factors are important for

the fractionation at hand. Nevertheless, for the purpose of discerning factors which can lead to improved separations, some of these concepts will be employed but their shortcomings must be kept in mind.

The chemical parameters influencing separation were discussed earlier. This section will deal with physical parameters. Two different K_D 's can be substituted in expressions for Q (eq. (26)) and the resulting equation solved for the tube number at the intersection point of the two curves. Nichols⁸¹ combined the resultant with the Gaussian approximation to the ideal distribution to obtain the following:

$$(36) \quad N = t^2 \left[\frac{\frac{K_D K_D}{K_D + 1} - 1}{\frac{1}{K_D} - \frac{1}{K_D} + 1} \right]^2$$

which gives the number of transfers required for the desired binary separation. Nomographs⁸² have been presented to simplify the estimation, but in this and similar treatments the phase volume ratio was taken as one, so that the effect of its variation often has been overlooked. For this reason N was usually considered along with c , that is increasing N involved increasing the distributor length. Alternatively, unresolved components can be fed back or recycled into the first tube and the fractionation continued.⁸³ This approach must be applied judiciously, of course, since in this closed system a solute with high K_D could catch up to one favoring the lower phase (equations (19) and (20)).

Grushka⁸⁴ applied the chromatographic concept of resolution (R_s) to countercurrent distribution and obtained the following expression:

$$(37) \quad R_s = \frac{(M_{\max 2} - M_{\max 1})}{2(\Sigma_2 + \Sigma_1)} = \frac{\frac{1}{2} \left(\frac{K_D_1}{K_D_1} (1 + sK_D_2) - \frac{K_D_2}{K_D_2} (1 + sK_D_1) \right)}{\left(\frac{K_D_1}{K_D_1} \right)^{\frac{1}{2}} (1 + sK_D_2) + \left(\frac{K_D_2}{K_D_2} \right)^{\frac{1}{2}} (1 + sK_D_1)}$$

After differentiation with respect to the solvent (*s*) and setting the derivative equal to zero, the well known Bush-Densen⁸⁵ relation (eq. (38)) was obtained. This relation:

$$(38) \quad s = \left(K_{D_1} K_{D_2} \right)^{-\frac{1}{2}}$$

was originally derived for a specific distribution pattern, i.e., where *c* stages and only batches of each phase were used. However, it has frequently been applied to CCD in general.^{86,87} In the above derivation the number of transfers was constant.

The number of transfers before a given small amount of solute leaves the distributor is:⁷⁷

$$(39) \quad M_{\max} = c - 1 - t \Sigma .$$

Combination of equations (39) (for faster moving component), (37) and (20) yielded an expression for R_s in which *N* is variable.

$$(40) \quad R_s = \frac{\left(\sqrt{t^2 + 4(R - 1)} \left(1 + sK_{D_1} \right) - t \right) \left(K_{D_1} - K_{D_2} \right)}{4 \sqrt{K_{D_1} K_{D_2}} \left(1 + sK_{D_1} \right) + 4 K_{D_1} \left(1 + sK_{D_2} \right)} .$$

Evaluation of this equation showed that for the usual situation where for neighboring peaks, $K_{D_2} < 4 K_{D_1}$, decreasing *s* increased R_s .

For the single withdrawal approach,

$$(41) \quad R_s = \frac{c^{\frac{1}{2}} \left(K_{D_1} - K_{D_2} \right)}{2 K_{D_1} \left(sK_{D_2} + 1 \right)^{\frac{1}{2}} + 2 K_{D_2} \left(sK_{D_1} + 1 \right)^{\frac{1}{2}}} .$$

Clearly, decreasing the solvent ratio leads to increased resolution of a given solute pair when *c* is constant. Results of a 50 tube simulated, ideal distribution are given in Table V.⁷⁷ Total percent impurity, TPI, is also shown as a criterion of separation and is defined in the glossary. The intersection of the distribution profiles was taken as the cutpoint between the regions.

TABLE V
Effect of Solvent Volume Ratios^a

Inside				Single Withdrawal		
s	N	TPI	R _s	N	TPI	R _s
0.8	72	39.0	0.41	141	30.8	0.51
0.5	89	35.4	0.44	193	26.0	0.54
0.125	229	29.8	0.54	602	18.3	0.65

^a c = 50 K_{D1} = 1.5, K_{D2} = 1.0

This cutpoint maximizes the amount of each component found in its respective zone.

An unresolved solute pair was chosen to demonstrate the effect. Obviously complete separation could not be obtained with 50 tubes. By setting R_s = 1 and s = 0 in equation (41), a lower bound for c can be found:

$$(42) \quad c = \left(\frac{2 K_{D_2} + 2 K_{D_1}}{K_{D_1} - K_{D_2}} \right)^2.$$

For K_{D1} = 1.5, K_{D2} = 1.0, the lower bound is 100, while 150 would be a realistic choice. After solving equation (41) for s and making some simplifying assumptions, an approximation of the solvent ratio to give R_s = 1 is obtained:

$$(43) \quad s = \frac{\left(\frac{K_{D_1} - K_{D_2}}{K_{D_1} + K_{D_2}} \right)^2}{\left(\frac{K_{D_1} + K_{D_2}}{K_{D_1} - K_{D_2}} \right)^{\frac{1}{2}}}.$$

The plot shown in Figure 18 for the system K_{D1} = 1.5, K_{D2} = 1.0 and c = 150 demonstrates that a R_s of one is well within reason. A solvent ratio of 0.42 was calculated using equation (43).

In practice, the options of manipulating c or s or both must be considered. Often it is not convenient to select any desired

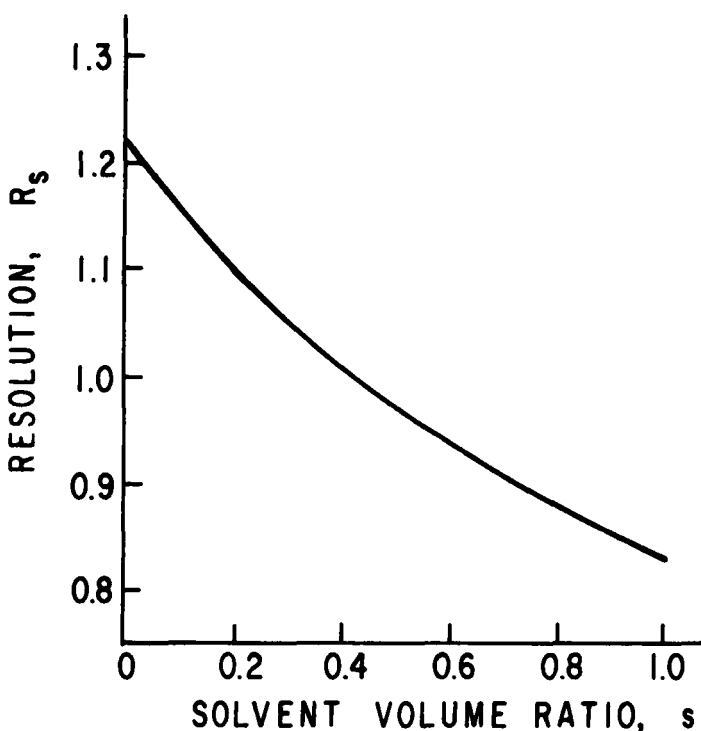


FIGURE 18
Effect of solvent-volume ratio on resolution

number of tubes because of the construction of automated apparatus so that compromises must be made. The disadvantages of lower s include lengthened separation time, increased concentration-related effects, and increased alteration of the separation by such factors as the V_U retained term in Figure 9.

Nonideal effects can be minimized by dividing a larger solute charge into a number of batches and placing these in the first tubes of the distributor. It has been suggested that up to 5% of the tubes⁸⁸ or the number of tubes equal to 7% of the total number of transfers⁸⁹ applied could be filled in this manner without significantly altering the separation. However, the sequential-input approach described earlier seems to be a better alternative.⁹⁰

A comparison is made in Figure 19 where unit inputs were either made on each transfer for the stated number or placed in the stated number of tubes. About thirty inputs could be made sequentially and would give the same separation as only ten tubes batchloaded. Batchloading essentially decreases the number of tubes while each input made sequentially contacts each tube. Barford⁶² showed that when enough inputs are made to produce frontal outputs under ideal conditions the number of tubes required for a given separation is:

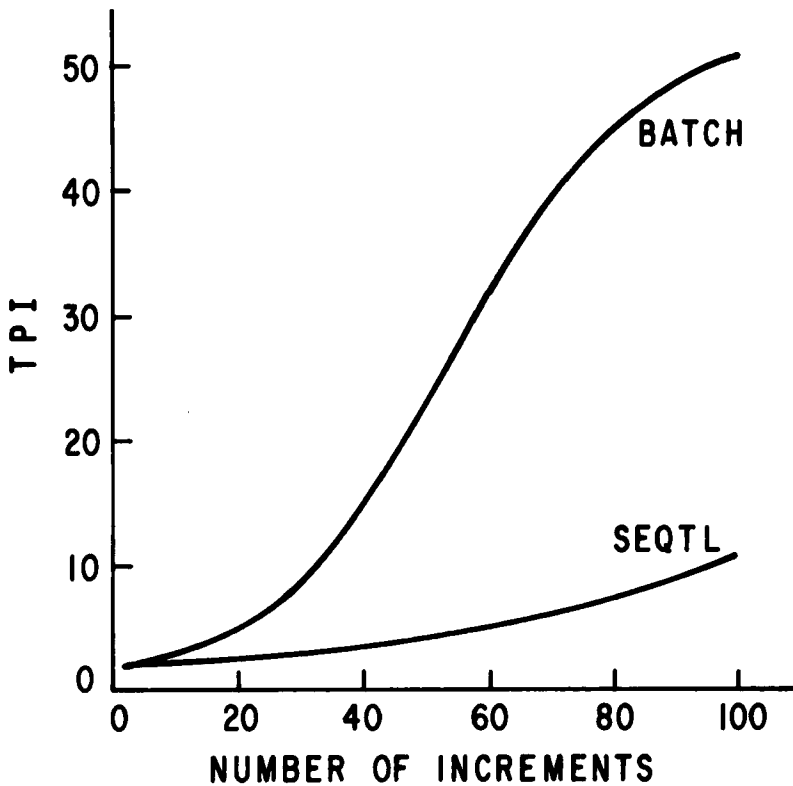


FIGURE 19
Effect of method of sample loading.
 $K_{D1} = 1.5$, $K_{D2} = 1.0$, $c = 200$, $V_U = 20$, $V_L = 40$

$$(44) \sqrt{c} = \frac{(4.66 - t_{i,2}) K_{D_1} \sqrt{1 + K_{D_2} s} + t_{i,1} \sqrt{1 + K_{D_1} s}}{K_{D_1} - K_{D_2}}$$

Preparative separations by CDCCD are usually performed using the steady state mode so that one solute is isolated in high yield and purity while the others, all of either higher or lower K_D , collected in the other phase. Optimization then reduces to selecting the best conditions for resolving the desired product from its nearest neighbor.

The relationships which Scheibel⁹¹ derived from stagewise continuous extraction may also be applied to CDCCD, assuming constant K_D , and s , large c_R and c_L , and no solvent is added with solute. At steady state one solvent ratio requires fewer tubes for a given separation than any other. This ratio is:

$$(45) \log s K_{D_1} = \frac{\log K_{D_1} / K_{D_2}}{1 + \left(\frac{\log E_2}{\log E_1} \right)^{\frac{1}{2}}}$$

where $E_i = (Y_i) / (1 - Y_i)$.

The fractions extracted in the phases, Y_i and $(1 - Y_i)$ are determined from the separation requirements in terms of amount of product per transfer and its purity. The number of stages required at this s is:

$$(46) c = \frac{2 \log E_1 E_2}{\log K_{D_1} K_{D_2}} \left(1 - 0.4 \left| \log \frac{E_1}{E_2} \right| \right)$$

while the feed tube position is given by:

$$(47) \frac{c_R}{c_L} = \left(\frac{\log E_2}{\log E_1} \right)^{\frac{1}{2}} \left(1 + \frac{\log \frac{E_1}{E_2}}{E_2 \log E_1} \right)$$

where $E_2 < E_1$ and upper phase moves to right. When solute is fed into the center, the Bush and Densen relation is optimal.

Treybal⁹² states that these expressions give nearly correct, although not exact results. As in CCD, computer simulation gives greater flexibility⁹³ and permits nonideal effects to be considered.

SUMMARY

Although modern high performance liquid chromatography has replaced liquid-liquid extraction for most analytical separations, the latter is widely used for sample "cleanup" and, most advantageously, for preparative separations on a scale between chromatography and plant-size continuous extractors. Discontinuous extraction, in all its forms and modes of operation, is particularly well suited to the separation of labile biological materials. New insights into the nature of the countercurrent process have led to new procedures for increasing solute throughput and degree of separation. New approaches have been developed for predicting liquid equilibria but these data fitting methods offer little, if any, advantage over completely experimental methods. However, research continues in this important area as shown, for example in Reference 94.

ACKNOWLEDGMENT

The author thanks Herbert L. Rothbart for his helpful discussions.

REFERENCES

1. W. L. Lewis and W. L. Martin, *Hydrocarbon Process.*, 46, 131 (1967).
2. L. F. Mayhue, "Solvent Extraction Status Report," *Environ. Prot. Technol. Ser.*, EPA-R2-72-073 (1972).
3. M. Beroza and M. C. Bowman, *J. Amer. Oil Chem. Soc.*, 48, 358 (1965).
4. S. J. Romano, K. H. Wells, H. L. Rothbart, and W. Rieman III, *Talanta*, 16, 581 (1969).

5. Proc. Int. Solvent Extraction Conf. The Hague. The Society of Chem. Industry, London (1971).
6. J. Ingham, Rep. Progr. Appl. Chem., 57, 267 (1973).
7. G. G. Pollock and A. I. Johnson, Ion Exch. Solvent Extn., 6, 59 (1974).
8. P. K. Hietala, Acta Chim. Scand., 14, 212 (1960).
9. M. M. Anwar, C. Hanson, and M. W. T. Pratt, Chem. Ind., (London), 1090 (1969).
10. P. Winistorfer and E. Kovats, J. Gas Chromatogr., 5, 362 (1967).
11. S. C. Pan, Separ. Sci., 9, 227 (1974).
12. Y. Ito, R. E. Hurst, R. L. Bowman, and E. K. Achter, Sep. Purif. Methods, 3, 133 (1974).
13. L. C. Craig and O. Post, Anal. Chem., 21, 500 (1949).
14. O. Post and L. C. Craig, ibid., 35, 641 (1963).
15. F. C. Alderweireldt, ibid., 33, 1920 (1961).
16. H. A. Wilhelm and R. A. Foos, Ind. Eng. Chem., 51, 633 (1959).
17. R. Signer and H. Arm. Helv. Chim. Acta, 50, 46 (1967).
18. P. Å. Albertsson, "Partition of Cell Particles and Macromolecules," 2nd Ed., Wiley-Interscience, New York (1972).
19. C. Galeffi, J. Chromatogr., 92, 1 (1974).
20. G. Blomquist and S. Wold, Acta Chem. Scand., Ser. B, 28, 56 (1974).
21. A. Jeney and B. W. Fox, Chem-Biol. Interact., 7, 265 (1973).
22. W. Gerhardt, V. P. Harigopal, and S. Suss, J. Amer. Oil Chem. Soc., 51, 479 (1974).
23. J. W. Gibbs, Trans. Conn. Acad. Arts Sci., 3, 108 (1875).
24. F. Duhem, Comptes Rendu, 102, 1449 (1886).
25. J. H. Hildebrand and R. L. Scott, "Regular Solutions," Prentice-Hall, Inc., Englewood Cliffs, N. J. (1962).

26. R. A. Barford, R. J. Bertsch, and H. L. Rothbart, *J. Amer. Oil Chem. Soc.*, 45, 141 (1968).
27. P. C. Wankat, *J. Chromatogr.*, 88, 211 (1974).
28. C. A. Hollingsworth, J. J. Taber, and B. F. Daubert, *Anal. Chem.*, 28, 1901 (1956).
29. R. E. Treybal, "Liquid Extraction," 2nd Ed., McGraw-Hill, New York (1963), p. 10.
30. L. S. Palatnik and A. I. Landau, "Phase Equilibria in Multi-component Systems," Holt, Rinehart, and Winston, New York (1964).
31. J. F. Rusling, R. J. Bertsch, R. A. Barford, and H. L. Rothbart, *J. Chem. Eng. Data*, 14, 169 (1969).
32. J. W. Gibbs, *Trans. Conn. Acad. Arts Sci.*, 3, 152 (1876).
33. A. W. Francis, "Liquid-Liquid Equilibria," Interscience, New York (1963).
34. K. Wohl, *Trans. Am. Inst. Chem. Engrs.*, 42, 215 (1946).
35. O. Redlich and A. T. Kister, *Ind. Eng. Chem.*, 40, 345 (1948).
36. G. M. Wilson, *J. Am. Chem. Soc.*, 86, 127 (1964).
37. H. Renon and J. M. Prausnitz, *A.I.Ch.E.J.*, 14, 135 (1968).
38. J. F. Heil and J. M. Prausnitz, *ibid.*, 12, 678 (1966).
39. J. M. Prausnitz, C. A. Eckert, R. V. Orye, and J. P. O'Connell, "Computer Calculations for Multicomponent Vapor-Liquid Equilibria," Prentice-Hall, Inc., Englewood Cliffs, N. J. (1967).
40. J. W. Hudson and M. Van Winkle, *J. Chem. Eng. Data*, 14, 310 (1969).
41. J. H. Hildebrand and R. L. Scott, "Solubility of Non-Electrolytes," 3rd Ed., Dover Pubs., Inc., New York (1964).
42. H. Burrell, *Offic. Dig. Fed. Paint Varn. Prod. Clubs*, 27, 726 (1955).
43. K. L. Hoy, *J. Paint Technol.*, 42, 76 (1970).
44. P. A. Small, *J. Appl. Chem.*, 3, 71 (1953).
45. D. E. Martire and D. C. Locke, *Anal. Chem.*, 43, 68 (1971).

46. H. M. N. H. Irving, *Ion Exch. Solvent Extr.*, 6, 139 (1974).
47. R. L. Scott, *Ann. Rev. Phys. Chem.*, 7, 43 (1956).
48. S. S. Davis, T. Higuchi, and J. H. Rytting, *Adv. Pharm. Sci.*, 4, 73 (1974).
49. S. S. Davis, *Separ. Sci.*, 10, 1 (1975).
50. M. J. Harris, T. Higuchi, and J. H. Rytting, *J. Phys. Chem.*, 77, 2694 (1973).
51. H. Freiser in "An Introduction to Separation Science," B. L. Karger, L. R. Snyder, and C. Horvath, Eds. J. Wiley & Sons, New York (1973), p. 247.
52. "Solvent Extraction Chemistry," Proc. of Int. Conf. at Gothenburg, Sweden, 1966. North Holland Pub. Co., Amsterdam (1967).
53. E. Soczewinski in "Advances in Chromatography," Vol. 8, J. C. Giddings and R. A. Keller, Eds. Marcel Dekker, Inc., New York (1969), p. 97.
54. D. K. K. Liu, D. T. Shioshita, and R. L. McDonald, *J. Phys. Chem.*, 78, 2572 (1974).
55. C. R. Scholfield, E. P. Jones, R. O. Butterfield, and H. J. Dutton, *Anal. Chem.*, 35, 1588 (1963).
56. L. C. Craig, *J. Biol. Chem.*, 150, 33 (1943).
57. L. C. Craig and D. Craig in "Techniques of Organic Chemistry," A. Weissberger, Ed., Vol. III, Interscience Publishers, New York (1950), p. 193.
58. L. C. Craig, W. Hausmann, E. H. Ahrens, Jr., and E. J. Harfenist, *Anal. Chem.*, 23, 1236 (1951).
59. D. G. Therriault and R. H. Poe, *Can. J. Biochem.*, 43, 1427 (1965).
60. H. L. Rothbart, R. A. Barford, V. G. Martin, R. J. Bertsch, and C. R. Eddy, *Separ. Sci.*, 4, 325 (1969).
61. R. McGraw, R. A. Barford, and H. L. Rothbart, Abstracts of Middle Atlantic Regional Meeting, Am. Chem. Soc., Philadelphia, Pa. (1972). Manuscript in press.
62. R. A. Barford, H. L. Rothbart, and R. J. Bertsch, *Separ. Sci.*, 6, 175 (1971).

63. R. C. Williams, Jr., and L. C. Craig, ibid., 2, 487 (1967).
64. V. G. Martin, R. A. Barford, C. R. Eddy, and H. L. Rothbart, Computer Programs for Countercurrent Distribution, U. S. Department of Agriculture ARS-73-63 (1969).
65. R. H. Purdy, N. L. Goldman, and G. S. Richardson, J. Biol. Chem., 240, 1573 (1965).
66. R. L. Priore and R. Y. Kirdani, Anal. Biochem., 24, 360 (1968).
67. S. Stene, Ark. Kemi, Mineral. Geol., 18A, 1 (1944).
68. N. E. Day, Ind. Eng. Chem. Fundam., 5, 499 (1966).
69. E. L. Compere and A. L. Ryland, Ing. Eng. Chem., 46, 24 (1954).
70. H. J. Dutton, R. O. Butterfield, and A. Rothstein, Anal. Chem., 38, 1773 (1966).
71. C. R. Schofield, R. O. Butterfield, and H. J. Dutton, Lipids, 1, 163 (1965).
72. R. E. Treybal, "Liquid Extraction," 2nd Ed., McGraw-Hill, New York (1963), p. 372.
73. T. R. C. Boyde, Separ. Sci., 6, 771 (1971).
74. E. Glueckauf, Trans. Faraday Soc., 51, 34 (1955).
75. A. S. Said, J. Gas Chromatogr., 1, (6), 20 (1963).
76. K. Rietema, Chem. Eng. Sci., 7, 89 (1957).
77. V. G. Metzger, R. A. Barford, and H. L. Rothbart, Separ. Sci., 8, 143 (1973).
78. P. R. Rony, Separ. Sci., 3, 239 (1968).
79. H. Svensson, J. Chromatogr., 25, 266 (1966).
80. K. de Clerk and C. E. Cloete, Separ. Sci., 6, 627 (1971).
81. P. L. Nichols, Jr., Anal. Chem., 22, 915 (1950).
82. J. A. D. Jeffreys, Chem. Ind. (London), 1594 (1967).
83. L. C. Craig and D. Craig in "Techniques of Organic Chemistry," A. Weissberger, Ed., Vol. III, Interscience Publishers, New York (1950), p. 200.

84. E. Grushka, *Separ. Sci.*, 7, 293 (1972).
85. M. T. Bush and P. M. Densen, *Anal. Chem.*, 20, 121 (1948).
86. L. C. Craig and D. Craig in "Techniques of Organic Chemistry," A. Weissberger, Ed., Vol. III, Interscience Publishers, New York (1950), p. 179.
87. C. J. O. R. Morris and P. Morris, "Separation Methods in Biochemistry," Interscience Publishers, New York (1963), p. 566.
88. L. C. Craig and D. Craig in "Techniques of Organic Chemistry," A. Weissberger, Ed., Vol. III, Interscience Publishers, New York (1950), p. 149.
89. T. P. King and L. C. Craig, *Methods of Biochemical Analysis*, D. Glick, Ed., Vol. X, Interscience Publishers, New York, p. 217.
90. V. G. Martin and R. A. Barford, *Abstracts of 161st National Meeting, American Chemical Society, Los Angeles (1971)*. Manuscript in press.
91. E. G. Scheibel, *Ind. Eng. Chem.*, 46, 16 (1954).
92. R. E. Treybal, "Liquid Extraction," 2nd Ed., McGraw-Hill, New York (1963), p. 328.
93. R. O. Butterfield, C. K. Tjarks, and H. J. Dutton, *Anal. Chem.*, 39, 497 (1967).
94. D. S. Abrams and J. M. Prausnitz, *A.I.Ch.E.J.*, 21, 116 (1975).

GLOSSARY

a = activity

(1-A) = fraction of solute transferred

c = number of tubes in distributor

D_C = molar concentration of all C-containing species in phase 2/molar concentration of C^{Z+} ions in phase 1

E = fraction extracted in upper phase/fraction in lower = $Y/(1-Y)$

f = mole fraction activity coefficient

F_N = fraction of solute in output at transfer N, single input

$F_{N,k}$ = fraction in output, multiple input
 F_{MAX} = fraction at maximum, multiple input
 F = fraction in output, frontal
 F_{SS} = fraction in output at steady state
 G_i = Gibbs energy of component i
 ΔG^m = Gibbs energy of mixing
 g_{ji} = interaction energy between two species
 ΔH_v = heat of vaporization
 I = terms in Van Laar equations
 K = distribution coefficient, mole fraction in phase 2/
mole fraction in phase 1
 K_D = distribution coefficient, moles per liter in phase 2
(upper)/moles per liter in phase 1
 L_1 = tie line segment from composition of phase 1
 L_2 = tie line segment from composition of phase 2
 M = tube number
 n = number of moles
 N = transfer number
 N_U = upper phase transfer
 N_L = lower phase transfer
 N_R = number of transfers to eluted peak max.
 N_{RF} = number of transfers to half height of step function
 P = pressure
 P_1 = mass of phase 1
 P_2 = mass of phase 2
 r = particle radius
 R = gas constant
 R_s = resolution
 S = adjustable parameter
 s = volume of upper phase/volume lower phase
 T = temperature
 TPI = mole percent of component 2 contaminating component 1
fraction + percent of component 1 in component 2
fraction

t = ordinate of cumulative normal distribution,

$$F = \frac{1}{2\pi} \int_{N=0}^N \exp = \frac{t^2}{2} dt \cdot \text{In CCD, } t = (N - N_{Ro})/\Sigma_o$$

t_1 = value of t at intersection of two curves, 1 and 2

V = molar volume

V_U, V_L = volumes of upper and lower phase

v = fraction of upper phase retained in cell

w_i = weight fraction of i in phase

W_i = total weight fraction of i in system

x = mole fraction

Y = fraction of solute extracted into upper phase =

$$s K_D / (s K_D + 1)$$

z = fraction of lower phase transferred

Z = charge

α_{ij} = nonrandomness constant

ϕ_i = volume fraction of component i in solution

σ = solubility parameter or cohesive energy

β_C = fraction of all C -containing species in phase 1 that are in C^{Z+} form

Σ_o = standard deviation of output profile

Σ = standard deviation of band inside distributor

τ = adjustable parameter

φ = constant in eq. (11), either 0 or 1 as stated

$\mu_{i,i}$ = chemical potential of component i in phase 1

μ_0 = chemical potential of pure component

ψ = constant in eq. (11), either 0 or 1 as stated

$\#$ = number of last component

$\tau_{i,L}$ = interfacial tension between particles and lower phase in phase 1

$[i,1]$ = molar concentration in phase 1